

A Novel Calibration Method for Active Interferometer-Based VNAs

Mubarak, F. A.; Romano, R.; Rietveld, G.; Spirito, M.

DOI

[10.1109/LMWC.2020.3006701](https://doi.org/10.1109/LMWC.2020.3006701)

Publication date

2020

Document Version

Final published version

Published in

IEEE Microwave and Wireless Components Letters

Citation (APA)

Mubarak, F. A., Romano, R., Rietveld, G., & Spirito, M. (2020). A Novel Calibration Method for Active Interferometer-Based VNAs. *IEEE Microwave and Wireless Components Letters*, 30(8), 829-832. Article 9139196. <https://doi.org/10.1109/LMWC.2020.3006701>

Important note

To cite this publication, please use the final published version (if applicable). Please check the document version above.

Copyright

Other than for strictly personal use, it is not permitted to download, forward or distribute the text or part of it, without the consent of the author(s) and/or copyright holder(s), unless the work is under an open content license such as Creative Commons.

Takedown policy

Please contact us and provide details if you believe this document breaches copyrights. We will remove access to the work immediately and investigate your claim.

A Novel Calibration Method for Active Interferometer-Based VNAs

F. A. Mubarak¹, Member, IEEE, R. Romano, G. Rietveld², Senior Member, IEEE, and M. Spirito, Member, IEEE

Abstract—The addition of RF interferometers to vector network analyzer (VNA) test benches has allowed for realization of low-noise high-frequency measurements of extreme impedance devices. However, when employing correction techniques such as the short-open-load method, the RF response of the interferometer hardware introduces measurement inaccuracies due to unwanted load-dependent inconsistencies. This letter presents a novel VNA calibration method that enables both low-noise and accurate small-signal characterization of highly mismatched devices. The proposed solution is experimentally validated in the 10–18-GHz band, confirming a 23-fold improvement in measurement resolution with absolute accuracy across the entire Γ range of the VNA. The accuracy of the new calibration process is verified via comparison with traceable reference standards supported by state-of-the-art uncertainties.

Index Terms—Calibration, extreme impedance measurement, impedance mismatch, measurement, microwave interferometry, nanoelectronics, nanostructures, noise, traceability, vector network analyzer (VNA).

I. INTRODUCTION

VECTOR network analyzers (VNAs) are considered as the most accurate instruments for small-signal characterization of devices in the GHz and THz frequency range. Introduced as a scalar impedance meter in the 1950s, the VNA has advanced into a sophisticated research and development instrument supporting linear, nonlinear, load-pull, pulsed, power, noise, and time-domain measurements. Recent works [1]–[6] have enhanced the measurement resolution of VNAs and offer a novel solution to a considerable hinder in the characterization of highly mismatched materials and devices [7]–[9]. This is realized through zeroing the measured input reflection coefficient (S_{11}^m) by employing an RF interferometer in the VNA test bench.

The measurement accuracy of extreme impedances (i.e., devices exhibiting $|S_{11}| \approx 1$) is subject to two dominant uncertainty contributions: the absolute measurement accuracy, set by the uncertainty of calibration standards, and the relative measurement accuracy (resolution), predominantly determined

by VNA noise behavior under the mismatched loading conditions [5], [10]. As the interferometer becomes an integral part of the VNA measurement system, it needs to support calibration across the entire S_{11}^m measurement range (i.e., $0 < |S_{11}^m| < 1$) and retain the ability to zero S_{11}^m for achieving a high measurement resolution.

Previous works [2]–[5] have demonstrated the capability to enhance the VNA measurement resolution in highly mismatched loading conditions using active interferometer solutions. A two-step calibration procedure is employed to realize absolute measurement accuracy. First, the interferometer is disabled (so-called “off”-mode), and the short-open-load (SOL) calibration procedure is used to calculate error terms of the system. Here, the interferometer does not inject a signal into the measurement path. In the second step, the interferometer is set in the so-called “on”-mode by injecting a separate signal into the measurement path. Here, S_{11}^m is zeroed using a known impedance reference standard (IRS) to renormalize the characteristic impedance of the calibration. Finally, the device under test (DUT) measurement data are acquired in on-mode with interferometer settings kept identical to those during IRS measurement and corrected using the off-mode error terms of the system. It is worth noting that this calibration technique only holds if the error terms of the measurement system do not change during the “on”- and “off”-mode measurements. However, none of the previous works has established the validity of this assumption across the entire S_{11}^m measurement range. Hence, a significant source of uncertainty is not properly addressed. Only [6] attempted to assess the absolute measurement accuracy corresponding to the calibration of an active interferometer-based VNA test bench. However, this method is only valid for a DUT that closely resembles the reference impedance used during the calibration procedure.

In this letter, we present a novel interferometer topology and calibration method for VNAs based on an architecture that includes the measurement of the RF response (i.e., transfer function) of the interferometer hardware. This approach allows for active cancellation of unwanted discrepancies in the transfer function, ensuring that the error terms of the measurement system remain constant throughout the entire experiment. The proposed method allows for calibration across the full S_{11}^m VNA measurement range and is experimentally validated through broadband calibration (10–18 GHz) of highly mismatched coaxial devices. We present the successful validation of the absolute accuracy of the proposed system by comparison with traceable reference values and, furthermore, show an improvement of factor 23 in resolution for the proposed system compared with a conventional VNA.

Manuscript received April 26, 2020; accepted June 12, 2020. Date of publication July 13, 2020; date of current version August 7, 2020. This work was supported by the Dutch Ministry of Economic Affairs. (Corresponding author: F. A. Mubarak.)

F. A. Mubarak and G. Rietveld are with the Department of Research and Development, National Metrology Institute of The Netherlands (VSL), 2629 JA Delft, The Netherlands (e-mail: fmubarak@vsl.nl).

R. Romano is with Vertigo Technologies B.V., 2629 JA Delft, The Netherlands.

M. Spirito is with the Electronics Engineering Department, Delft University of Technology (TUD), 2629 JA Delft, The Netherlands.

Color versions of one or more of the figures in this letter are available online at <http://ieeexplore.ieee.org>.

Digital Object Identifier 10.1109/LMWC.2020.3006701

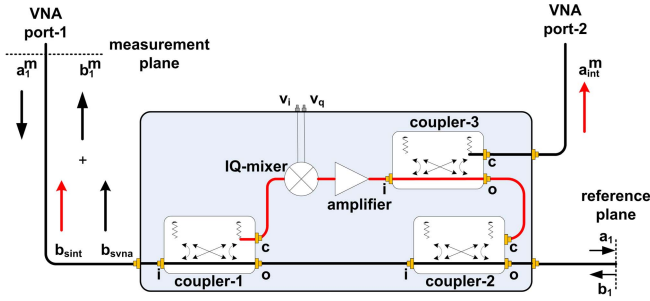


Fig. 1. Simplified block diagram of the proposed active interferometer-based VNA for extreme-impedance measurements.

II. PRINCIPLE OF OPERATION

The configuration of the proposed active interferometer-based VNA is schematically shown in Fig. 1. The key novelty in the setup design is reflected in simultaneous measurement of the input reflection coefficient S_{11}^m and the interferometer-induced signal a_{int}^m at VNA port-2. The measured input reflection coefficient S_{11}^m is defined as

$$S_{11}^m = \frac{b_1^m}{a_1^m} \quad (1)$$

where a_1^m is the incident and b_1^m is the scattered wave measured at port-1 of the VNA. The proposed system uses two incident signals for a measurement

$$S_{11}^m = \frac{b_{svna}}{a_1^m} + \frac{b_{sint}}{a_1^m} = S_{11,svna} + H(v_i, v_q)S_{11,sint}. \quad (2)$$

Here, $S_{11,svna}$ describes the uncorrected reflection coefficient realized by the scattered wave b_{svna} when stimulating the DUT with a_1^m and no signal is injected by the interferometer (i.e., $H(v_i, v_q) = 0$, with $H(v_i, v_q)$ being the complex transfer function of the interferometer). The $H(v_i, v_q)S_{11,sint}$ term corresponds to the uncorrected reflection coefficient caused by interferometer induced a_{int}^m , as shown in Fig. 1. For this, the coupled a_1^m is vector modulated by $H(v_i, v_q)$ using the quadrature mixer and subsequently injected into the measurement path. This leads to the second scattered signal $b_{sint}(v_i, v_q)$ measured by the VNA, which in turn exhibits an unwanted sensitivity to DUT S_{11} due to the limited isolation between the c and o ports of coupler-1 and coupler-2. The wave injected by the interferometer is described as

$$a_{int}^m(v_i, v_q) = a_1^m H(v_i, v_q). \quad (3)$$

Two digital-to-analog converters (DACs) are used to generate dc, v_i , and v_q signals to drive the IQ-ports of the quadrature mixer for vector modulation, as shown in Fig. 1. As the interferometer operates between the measurement and reference plane, its RF characteristics are embedded in the error terms during calibration of the system. However, error-term-based correction techniques, such as the SOL method, require the RF response of all devices up till the reference plane to be DUT S_{11} insensitive. Unfortunately, this requirement does not hold for $H(v_i, v_q)$, which exhibits sensitivity toward DUT S_{11} , as explained earlier. From (2), it is evident that $H(v_i, v_q)$ is not canceled out in the S_{11}^m measurement and thus leads to

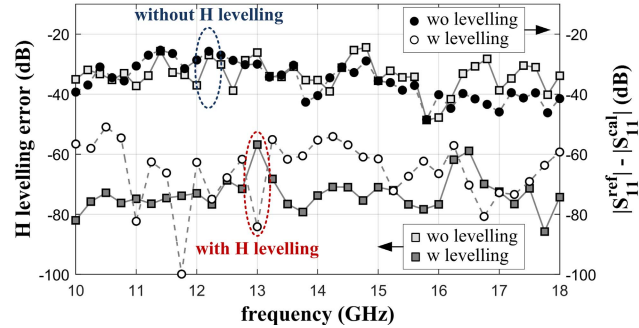


Fig. 2. Maximum vector difference between $H(v_i, v_q)$ values acquired during short, open, load, and offset-short device measurements (squares) as well as the difference between calibration and reference values for an offset-short device (DUT₂, circles). The top curves are acquired during conventional interferometer operation (without $H(v_i, v_q)$ levelling), whereas the bottom curves are collected by employing the proposed $H(v_i, v_q)$ leveling technique (see Section III for details).

errors. In practice, every variation in $H(v_i, v_q)$ caused by its sensitivity to S_{11} will directly propagate as a measurement error during the calibration process.

An experiment is proposed to quantify the variation of $H(v_i, v_q)$ and its impact on the measurement accuracy in broadband calibration of highly mismatched devices. A single-source interferometer [5] is used in conjunction with a Keysight VNA (PNA5225A) to calibrate two 3.5-mm coaxial precision offset-short devices ($\Gamma_{dut1,2}$) with metrology-grade SOL standards ($\Gamma_{ref1,2,3}$) in the 10–18-GHz range. Simultaneous to every S_{11}^m measurement, the corresponding $a_{int}^m(v_i, v_q)$ value is also acquired, allowing to determine $H(v_i, v_q)$ using (3). The sensitivity of H to S_{11} is quantified by calculating the maximum vector difference between all acquired $H(v_i, v_q)$ values for each measurement frequency, as shown in Fig. 2. The results demonstrate the variations in $H(v_i, v_q)$ in the order of -30 dB, which also directly sets the calibration accuracy limit. This is evident in the comparison between the calibration and reference values of DUT₂. The technique proposed in this letter based on the monitoring and automated leveling of $H(v_i, v_q)$, as detailed in Section III, reduces the fluctuation of H to better than -60 dB, also shown in Fig. 2.

III. CALIBRATION METHOD

The proposed calibration technique for interferometer-based VNAs, as shown in Fig. 1, consists of six steps.

- 1) *Step 1:* Select three reference impedance standards REF_{1,2,3} with known reflection coefficient values $\Gamma_{ref1,2,3}$. Connect the reference standard that best approaches Γ_{dut} ; we take this as REF₁.
- 2) *Step 2:* Zero $S_{11,ref1}^m$ by optimizing v_i and v_q using, e.g., a Newton–Raphson algorithm [11] embedded in the measurement software [5], with -70 dB for $S_{11,ref1}^m$ as threshold for completion of the zeroing process. Once $S_{11,ref1}^m$ has accomplished the zeroing limit, store the values $H_{ref1} = H(v_{i,ref1}, v_{q,ref1})$, $v_{i,ref1}$, and $v_{q,ref1}$.
- 3) *Step 3:* Connect the second reference standard REF₂ to the measurement port.

- 4) *Step 4*: Set $v_i = v_{i,\text{ref1}}$ and $v_q = v_{q,\text{ref1}}$ and measure $H(v_i, v_q)$.
- 5) *Step 5*: If $|H(v_i, v_q) - H_{\text{ref1}}|$ exceeds the error limit (set at -80 dB), reoptimize v_i and v_q until the error is smaller than this limit. In this way, leveling of the interferometer transfer function is realized by the Newton–Raphson algorithm, converging $H(v_i, v_q)$ toward H_{ref1} . Upon completion of this process, measure $S_{11,\text{ref2}}^m$ and store the values.
- 6) *Step 6*: Repeat Steps 3–5 for the remaining devices, REF₃ and DUT.

Once the measurements of $\Gamma_{\text{ref1,2,3}}$ are completed, the system error terms are calculated as follows:

$$\begin{bmatrix} e_{00} \\ e_{11} \\ \Delta \end{bmatrix} = \begin{bmatrix} 1 & \Gamma_{\text{ref},1} S_{11,\text{ref1}}^m & -\Gamma_{\text{ref},1} \\ 1 & \Gamma_{\text{ref},2} S_{11,\text{ref2}}^m & -\Gamma_{\text{ref},2} \\ 1 & \Gamma_{\text{ref},2} S_{11,\text{ref3}}^m & -\Gamma_{\text{ref},3} \end{bmatrix}^{-1} \begin{bmatrix} S_{11,\text{ref1}}^m \\ S_{11,\text{ref2}}^m \\ S_{11,\text{ref3}}^m \end{bmatrix} \quad (4)$$

with $\Delta = e_{11}e_{00} - e_{10}e_{01}$.

Here, e_{00} represents the directivity, e_{11} represents the source match, and $e_{10}e_{01}$ represents the reflection-tracking term of the measurement system. These are subsequently used to correct the DUT measurement S_{11}^m , resulting in S_{11} as follows:

$$S_{11} = \frac{S_{11}^m - e_{00}}{e_{10}e_{01} - e_{11}(S_{11}^m - e_{00})}. \quad (5)$$

IV. MEASUREMENT EXPERIMENTS AND DISCUSSION

This section examines the resolution (noise) and accuracy (systematic error) performance of an interferometer-based VNA used for broadband calibration of highly mismatched devices (DUT_{1,2}). The measurement experiment for 10–18-GHz range is detailed in Section II and used in conjunction with the procedure outlined in Section III. The final calibration results are compared with reference values having state-of-the-art uncertainties, traceable to the Swiss National Metrology Institute (METAS).

The best measurement resolution is achieved in close vicinity of the reference impedance used to zero the input reflection coefficient during Step 1 of the calibration process described in Section III. In the first experiment, DUT₁ is used to demonstrate the measurement resolution and is selected with a phase offset of less than 1.0° difference from REF₁ across the entire measurement range. The absolute accuracy across the entire Γ range of the VNA is evaluated using DUT₂ with a phase offset of 80° – 170° with respect to REF₁ over the measured frequency range.

The measurement results of both experiments are shown in Fig. 3. First, we demonstrate the measurement resolution of the interferometer-based VNA benchmarked to a conventional VNA using DUT₁. At each frequency, 100 measurement points are collected and the standard deviation of these points is used to quantify the measurement resolution. The results of Fig. 3 show a substantial improvement, of factor 23, in noise of the proposed system with respect to the conventional VNA. Next, the absolute accuracy of the proposed system is determined through a comparison between the DUT_{1,2} calibration results

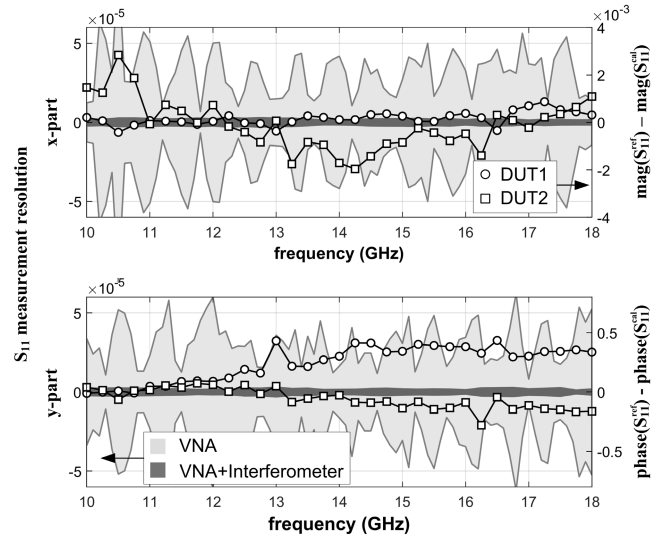


Fig. 3. S_{11} measurement resolution of the proposed interferometer-based VNA benchmarked to a conventional VNA (based on DUT₁ data), shown as dark- and light-gray areas, respectively (left axis). Difference between S_{11} calibration values for both offset-short devices DUT_{1,2} measured with the proposed interferometer-based VNA and reference values, shown by markers (right axis).

achieved through our new approach (S_{11}^{cal}) and METAS reference values (S_{11}^{ref}). The total uncertainty of the magnitude and phase reference values is 5×10^{-3} and 1.5° , respectively. The differences shown in Fig. 3 are substantially smaller than the corresponding uncertainty at all frequencies, for both verification devices. These results convincingly demonstrate the ability of the proposed hardware and calibration solution to realize a substantial improvement in measurement resolution and at the same time maintain absolute calibration accuracy across the entire Γ range of the VNA.

V. CONCLUSION

An accurate calibration method is presented for interferometer-based VNAs that allow for both low-noise and accurate small-signal characterization of highly mismatched devices. The core of the new method is an interferometer with simultaneous measurement of the injected signal and the input reflection coefficient parameters. The approach allows for readjustment of any discrepancy in the RF response of the interferometer. This ensures that the calibration error terms remain constant throughout all measurements, enabling accurate correction of these errors. Both attributes of the proposed system, calibration accuracy and measurement resolution, are experimentally validated and quantified. The results shown in Fig. 3 demonstrate an improvement of factor 23 in measurement resolution compared with a conventional VNA. The absolute accuracy is assessed by comparison of measurement results achieved by the new system with reference values, for two high-reflect offset-short devices selected to test the entire Γ range of the VNA. For both devices, all differences in measurement results are substantially smaller than the total measurement uncertainty of the reference values.

REFERENCES

- [1] K. Haddadi and T. Lasri, "Interferometric technique for microwave measurement of high impedances," in *IEEE MTT-S Int. Microw. Symp. Dig.*, Jun. 2012, pp. 1–3.
- [2] M. Randus and K. Hoffmann, "A method for direct impedance measurement in microwave and millimeter-wave bands," *IEEE Trans. Microw. Theory Techn.*, vol. 59, no. 8, pp. 2123–2130, Aug. 2011.
- [3] G. Vlachogiannakis, H. T. Shivamurthy, M. A. D. Pino, and M. Spirito, "An I/Q-mixer-steering interferometric technique for high-sensitivity measurement of extreme impedances," in *IEEE MTT-S Int. Microw. Symp. Dig.*, May 2015, pp. 1–4.
- [4] H. Votsi, C. Li, P. H. Aaen, and N. M. Ridler, "An active interferometric method for extreme impedance on-wafer device measurements," *IEEE Microw. Wireless Compon. Lett.*, vol. 27, no. 11, pp. 1034–1036, Nov. 2017.
- [5] F. A. Mubarak, R. Romano, L. Galatro, V. Mascolo, G. Rietveld, and M. Spirito, "Noise behavior and implementation of interferometer-based broadband VNA," *IEEE Trans. Microw. Theory Techn.*, vol. 67, no. 1, pp. 249–260, Jan. 2019.
- [6] R. Romano, F. Mubarak, M. Spirito, and L. Galatro, "The H-VNA, an interferometric approach for the accurate measurement of extreme impedances," in *Proc. 93rd ARFTG Microw. Meas. Conf. (ARFTG)*, Jun. 2019, pp. 1–6.
- [7] Z. V. Penfold-Fitch, F. Sfigakis, and M. R. Buitelaar, "Microwave spectroscopy of a carbon nanotube charge qubit," *Phys. Rev. A, Gen. Phys.*, vol. 7, no. 5, May 2017, Art. no. 054017.
- [8] V. Ranjan *et al.*, "Clean carbon nanotubes coupled to superconducting impedance-matching circuits," *Nature Commun.*, vol. 6, no. 1, pp. 1–6, May 2015.
- [9] D. Zhang *et al.*, "Simulation and measurement of optimized microwave reflectivity for carbon nanotube absorber by controlling electromagnetic factors," *Sci. Rep.*, vol. 7, no. 1, pp. 1–8, Mar. 2017.
- [10] F. Mubarak, R. Romano, and M. Spirito, "Evaluation and modeling of measurement resolution of a vector network analyzer for extreme impedance measurements," in *Proc. 86th ARFTG Microw. Meas. Conf.*, Dec. 2015, pp. 1–3.
- [11] T. J. Ypma, "Historical development of the Newton-Raphson method," *SIAM Rev.*, vol. 37, no. 4, pp. 531–551, Dec. 1995.